Journal of Heat and Mass Transfer Research

Journal homepage: http://jhmtr.journals.semnan.ac.ir

Semnan University

Mixed Convection Heat Transfer of Water-Alumina Nanofluid in an Inclined and Baffled C-Shaped Enclosure

Morteza Bayareh[a*], Mohammad Amin Kianfar[b], Abbas Kasaeipoor[c]

[a] *Department of Mechanical Engineering, Shahrekord University, Shahrekord, 88186- 34141, Iran.*
[b] *Department of Mechanical Engineering, Lamerd Branch, Islamic Azad University, Lamerd, Iran.*
[c] *Department of Mechanical Engineering, Isfahan University, Isfahan, Iran.*

PAPER INFO

Paper history:
Received: 2017-12-17
Received: 2018-05-19
Accepted: 2018-05-25

Keywords:
Mixed convection;
C-shaped enclosure;
Nanofluid;
Baffle.

ABSTRACT

In this article, mixed convection heat transfer of alumina-water nanofluid in an inclined and baffled C-shape enclosure is studied. It is assumed that the flow is laminar and steady. There is no energy production, energy storage and viscous heat dissipation. Furthermore, the nanofluid is considered as a continuous, Newtonian and incompressible fluid. Governing equations are discretized by finite-difference method and solved by SIMPLE algorithm simultaneously. Reynolds number ($10 < Re < 1000$), rotation angle of enclosure ($0° < \alpha < 90°$), length of baffle ($0.1 < Bf < 0.4$), Richardson number ($0.1 < Ri < 100$) are changed. In addition, volume percent of nanoparticles are changed in the range of $0 < \varphi < 0.06$. The results demonstrate that the Nusselt number increases with the Reynolds number. Adding nanoparticles always results in cooling enclosure. At high Reynolds number, increase of nanoparticles has less effect on the heat transfer rate than low ones. Finally, heat transfer increases with the Richardson number, the enclosure angle and the length of baffle.

DOI: 10.22075/jhmtr.2018.13390.1196

1. Introduction

Mixed convection heat transfer is of great interest to many researchers due to its wide application in different parts especially for cooling of electronic equipment, instruments of chemical processes and solar thermal collectors [1-5]. Siddik et al. [6] studied the effect of mixed heat transfer on the enclosure full of particles by using a lattice Boltzmann method. They examined their simulations by variation of Grashof number (1-400) and Reynolds number (50-1000). The results showed that the Grashof number has remarkable effect on the flow pattern and efficiency. Najm et al. [7] performed mixed convection heat transfer in a horizontal channel with a rectangular block distributed on the bottom wall periodically, while top wall was at constant low temperature. Their simulations were done for Reynolds numbers (0.1-200), Rayleigh numbers (10^2-10^6) and relative heights of block (0.25-0.5). Fully developed forced flow showed a reduction of heat transfer through cold level at high Reynolds numbers. Amin-ol-sadati and Ghasemi [8] studied mixed convection heat transfer in a horizontal enclosure with thermal source. They established whole range of Richardson numbers and dimensional ratios of enclosure. They found that at fixed Richardson number, the mechanism of heat transfer increases remarkably with increase of dimensional ratio at every three different states of hot source placement. When packet density increases in integrated electrical circuit board, an effective cooling process is necessary to gaurantee the satisfactory function of components of electrical board at high temperatures. Different strategies of innovative heat transfer were stated by Incropera [9], Patterson, and Ortega [10] experimentally and numerically.

In previous decades, mixed convection heat transfer is of interest to researchers of engineering sciences and

[*] *Corresponding Author: M. Bayareh, Department of Mechanical Engineering, Shahrekord University, Shahrekord, 88186- 34141, Iran.*
Email: m.bayareh@eng.sku.ac.ir

electronics industry. The main purpose of the studies has been finding different strategies to increase efficiency and cooling the excessive heat of electronic instruments with special geometry [11-14]. Alalemi et al. [15] studied the effect of blocks height with the same temperature on free convection heat transfer in a T-shape enclosure. Assessed parameters in this study were Rayleigh number, Prandtl number, and height of blocks. The results demonstrated that change of heat transfer with Rayleigh number is the same as that for smooth channels or vertical ribbed channels. Mezrhab et al. [16] studied the combination of free convection heat transfer and radiation in a T-shape enclosure. They studied the effect of block height, size of valve and Rayleigh number. Their results showed that when the enclosure height increases, average Nusselt number would increase. The Nusselt number increases if the radiation heat transfer is considered. Bakas et al. [17] examined free-convection heat transfer in a horizontal channel including heated rectangular blocks that were located on the lower wall periodically. Their results revealed that flow and heat transfer are dependent on the Rayleigh number, relative height of blocks and blocks distance from each other.

In recent years, study of nanofluid flow effects on heat transfer in an enclosure has attracted many attentions. Nanofluid flows contain particles in the size of nano. This liquid is colloidal suspension of nanofluid in a base fluid having more suspension stability than millimetre or micrometre sizes. Nanofluids have properties that make them helpful in many applications [18]. Therefore, it is expected that nanofluids increase heat transfer in comparison with pure liquids (e.g. water). This factor would allow the user to have heat or cool efficiently while energy consumption is reduced [19-21]. Pishkar and Ghasemi [22] studied the increase of mixed heat transfer by means of two fins attached to a horizontal channel saturated with nanofluid. They investigated the effect of Reynolds number, Richardson number, volume fraction of nanoparticles, and thermal conductivity of fins on the thermal performance. Their results indicated that the influence of volume fraction is remarkable at higher Reynolds numbers.

Mahmoudi et al. [23] studied the effect of entrance and exit on the mixed convection heat transfer in an enclosure for suitable ventilation exposed to external nanoparticles. This study was done for the Reynolds numbers (50-1000), Richardson numbers (0-10) and volume fractions of nanoparticles (0-0.05). The results showed that the nanoparticles have more effect on the functional improvement of heat transfer for high Reynolds and Richardson numbers in comparison with low ones.

Shahi et al. [24] studied mixed convection heat transfer of nanofluid flow in square enclosure. Their results showed that increase of concentration of nanoparticles results in the increase of average Nusselt number. Sortiji et al. [25] numerically established mixed convection heat transfer of aluminium-water nanofluid in a ventilated open enclosure with regard to different positions of exit. Their results demonstrated that the average Nusselt number depends on the Reynolds number, Richardson number and volume fraction. In addition, their research revealed that pressure drop coefficient increases with volume fraction of nanoparticles. Kasaei et al. [26] performed the numerical simulations of mixed convection heat transfer in a T-shape enclosure under magnetic field. They demonstrated that heat transfer increases with the Reynolds number, the Richardson number and volume fraction. Makulati et al. [27] investigated natural convection heat transfer of alumina-water nanofluid in an inclined C-shaped enclosure in the presence of magnetic field. Their results showed that the average Nusselt number decreases when the Hartmann number increases. In addition, as the non-dimensional ratio of the enclosure increases, the influence of the enclosure angle on the rate of heat transfer becomes less.

Recently, Siavashi et al. [28] investigated the effect of porous fins on natural convection in a cavity saturated by Cu-water nanofluid. They demonstrated that only porous fins with a high Darcy number can enhance the heat transfer rate. Siavashi and Rostami [29] studied the non-Newtonian nanofluid effect on natural convection heat transfer inside a cylindrical cavity with inner circular heat source. They also explored the influence of porous layer on the enclosure and revealed that it does not need fully porous cavity to obtain higher Nusselt number.

Mamourian et al. [30] obtained the optimum conditions for the mixed convective heat transfer in a wavy surface rectangular cavity saturated with nanofluid. They reported the optimum parametrs by using Taguchi method and found that wavy surface wavelength affects the heat transfer rate and entropy generation. For the case of wavy surface cavity, Milani Shirvan et al. [31] performed numerical simulations to study the wavy surface influence on natural convection heat transfer of a corrugated square cavity saturated with a nanofluid. They obtained the characteristics of the wavy surface and demonstrated that the Nusselt number increases as the volume fraction increases.

Convective heat transfer in enclosures include L-shaped and C-shaped ones has been applied in various industries such as solar energy systems and electronic chips. On the other hand, using nanoparticles suspended in a continuous liquid phase is a reasonable approach to enhance the heat transfer rate.

In the present study, mixed convection heat transfer of alumina-water nanofluid in a baffled and inclined C-shaped enclosure has been investigated. To the best of our knowledge, the effect of baffles on mixed convection heat transfer for the case of C-shaped enclosure has not been done in the presence of nanofluid. The results are presented to study the effect of Reynolds number, the rotation angle of enclosure, the volume fraction of nanoparticles, baffled length and the Richardson number on the rate of heat transfer.

2. Problem description

A two–dimensional C-shaped enclosure with a baffle in the middle of internal vertical wall is studied (Figure 1). Alumina-water nanofluid with the temperature, Tc and the velocity, uc enters from top right corner and exits the enclosure from the bottom right corner. Left vertical wall is considered at constant temperature. The baffles temperature is Tc. Aspect ratio is AR=H/L=0.3. The non-dimensional length of baffle is defined as Bf =a/L. The effect of different dimensionless parameters on the flow field and rate of heat transfer is also studied.

3. Governing equations

It is assumed that the flow is laminar and steady. There is no energy production, energy storage and viscous heat dissipation. Also, the nanofluid is considered as a continuous, Newtonian and incompressible fluid. By applying Boussinesq approximation, the governing equations (continuity, momentum and energy equations) are as follows, respectively [21, 26]:

$$\frac{\partial U}{\partial X}+\frac{\partial V}{\partial Y}=0 \tag{1}$$

$$U\frac{\partial U}{\partial X}+V\frac{\partial U}{\partial Y}=-\frac{\partial P}{\partial X}+\frac{\mu_{nf}}{\rho_{nf}\,\nu_f}\frac{1}{Re}\left[\frac{\partial^2 U}{\partial X^2}+\frac{\partial^2 U}{\partial Y^2}\right]+\frac{(\rho\beta)_{nf}}{\rho_{nf}\,\beta_f}Ri\;\theta\;\sin\alpha \tag{2}$$

$$U\frac{\partial V}{\partial X}+V\frac{\partial V}{\partial Y}-\frac{\partial P}{\partial Y}+\frac{\mu_{nf}}{\rho_{nf}\,\nu_f}\frac{1}{Re}\left[\frac{\partial^2 V}{\partial X^2}+\frac{\partial^2 V}{\partial Y^2}\right]+\frac{(\rho\beta)_{nf}}{\rho_{nf}\,\beta_f}Ri\;\theta\;\cos\alpha \tag{3}$$

$$U\frac{\partial \theta}{\partial X}+V\frac{\partial \theta}{\partial Y}=\frac{\alpha_{nf}}{\alpha_f}\frac{1}{Re\;Pr}\left[\frac{\partial^2\theta}{\partial X^2}+\frac{\partial^2\theta}{\partial Y^2}\right] \tag{4}$$

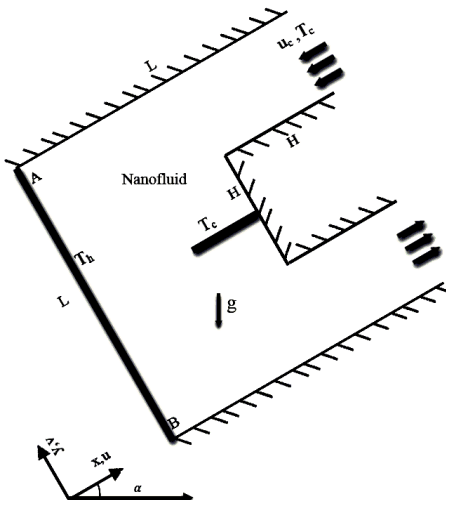

Figure 1. Schematic of the inclined C-shaped baffled enclosure.

Dimensionless variables used in the equations are as follows:

$X=\frac{x}{L}$, $Y=\frac{y}{L}$, $U=\frac{u}{v_0}$, $V=\frac{v}{v_0}$, $H=\frac{h}{L}$, $L_0=\frac{l_0}{L}$, $P=\frac{\overline{p}}{\rho_{nf}\,{v_0}^2}$, $\theta=\frac{T-T_C}{T_h-T_C}$

Also, Reynolds, Prandtl and Richardson numbers are defined as:

$$Re=\frac{v_0 L}{\nu_f},\quad Ri=\frac{Gr}{Re^2},\quad Pr=\frac{\nu_f}{\alpha_f} \tag{5}$$

where $\mathrm{Gr}=g\beta_{\mathrm{f}}(T_{\mathrm{h}}-T_{\mathrm{C}})L^3/{\vartheta_{\mathrm{f}}}^2$ is the Grashof number.

The Boundary conditions include no-slip condition on the wall of enclosure (U, V = 0), constant temperature at the walls ($\theta=1$) and for the entrance (V=0, U=1, $\theta=0$). Velocity components and the temperature at the baffle are V=0, U=0, and $\theta=0$, respectively. Furthermore, V=0, $\partial U/\partial Y=0$ and $\partial\,\theta\,/\partial Y=0$ are fully development condition for the exit of enclosure.

Amount of heat transfer is stated in the form of Nusselt number. Local Nusselt number on the hot wall is defined as:

$$Nu=-\frac{k_{nf}}{k_f}\left(\frac{\partial\theta}{\partial X}\right)_{X=0} \tag{6}$$

Average Nusselt number is calculated by integration of equation 6:

$$Nu_m=\frac{1}{L}\left[\int_0^1 Nu\;dY\right] \tag{7}$$

Density (ρ_{nf}), coefficient of volume expansion ($\rho\,\beta)_{nf}$, thermal capacity $(\rho c_p)_{nf}$, and thermal diffusivity coefficient $(\rho c_p)_{nf}$ of nanofluids are calculated by the following relations [32-33]:

$$\rho_{nf}=(1-\varphi)\rho_f+\varphi\rho_s \tag{8}$$

$$(\rho\beta)_{nf}=(1-\varphi)(\rho\beta)_f+\varphi(\rho\beta)_s \tag{9}$$

$$(\rho c_p)_{nf}=(1-\varphi)(\rho c_p)_f+\varphi(\rho c_p)_s \tag{10}$$

$$\alpha_{nf}=\frac{k_{nf}}{(\rho c_p)_{nf}} \tag{11}$$

The effective dynamic viscosity of nanofluids based on Brinkman relation [34] is presented below. It should be noted that this relation has been used by many researchers [2, 3, and 8]. They demonstrated that Brinkman model has a reasonable prediction for the same simulations as present one:

$$\mu_{nf}=\mu_f(1-\varphi)^{-2.5} \tag{12}$$

K_{nf} is the coefficient of thermal conductivity of nanofluids. For two independent components of spherical particles of suspension, this model is as follows:

$$k_{nf}=k_f\left[1+\frac{k_s A_s}{k_f A_f}+c k_s Pe\frac{A_s}{k_f A_f}\right] \tag{13}$$

Where k_s and k_f are coefficients of thermal conductivity of alumina- water nanofluids and pure fluid respectively. For alumina-water nanofluid, c=36000 is suggested [31]:

$$\frac{A_s}{A_f}=\frac{d_f}{d_s}\frac{\varphi}{1-\varphi} \tag{14}$$

The solid nanoparticles have a diameter equals to ds=100 nm and molecular size of water-based fluid is as follows:

$$d_f = 2\text{Å} \tag{15}$$

$$Pe = \frac{u_s d_s}{\alpha_f} \tag{16}$$

where u_s is the Brownian motion of a nanoparticle velocity:

$$u_s = \frac{2k_b T}{\pi \mu_f {d_s}^2} \tag{17}$$

where $k_b = 1.3807 \times 10^{-23}\ \text{JK}^{-1}$ is Boltzmann constant. Subscripts of nf, f, and s indicate nanofluid, fluid and solid nanoparticles, respectively. Prandtl number of pure water is

Table 1. Thermophysical properties of alumina nanoparticles and pure water [32- 33].

Thermo-physical properties	Pure water	Alumina nanoparticles
ρ (kgm-3)	997.1	3970
Cp (Jkg-1K-1)	4179	765
k (Wm-1K-1)	0.613	40
×105 (K-1)β	21	0.85

considered Pr = 6.2. Table 1 shows the thermophysical properties of water and alumina.

In order to model the intended geometry, a program was written in FORTRAN. Governing equations along with stated border conditions were algebralized by finite difference method based on the volume control. In order to handle the pressure-velocity coupling, the SIMPLE algorithm was employed. The power law discretization scheme was used to determine the convective fluxed across the surface of the control volume. It should be noted that many researchers employed the SIMPLE algoritm for Richardson numbers ranged from 0.1 to 10 [8]. In addition, the following convergence criteria were used:

$$\sum_j \sum_i \sqrt{\left[\left.\frac{\delta^{n+1} - \delta^n}{\delta^{n+1}}\right|_{i,j}\right]^2} \leq 10^{-8} \tag{18}$$

where, n and δ indicate the number of repetition and common variable of (U, V, Θ) respectively.

In order to validate the code, current results are compared with the results of Mahmoodi and Hashemi [35] and the results of Shahi et al. [24]. Figure 2 shows the average Nusselt number as a function of volume fraction at $Ra = 10^5$ for different aspect ratios compared to the results of Mahmoodi and Hashemi [35]. They examined the heat transfer rate in a C-shaped enclosure saturated with nanofluid. This figure confirms a very good agreement between the results. The maximum error is less than 1%. Shahi et al. [24] considered the mixed convective heat transfer in an open square cavity with nanofluid flow. Average Nusselt number versus volume fraction for different Richardson numbers at Re=100 is shown in Figure 3 in comparison with their results. The results are calculated for a square enclosure with nanofluid flow and a fixed flux on the floor. It is observed that current results are acceptable with good accuracy in comparison with the results of Shahi et al. [24]. It is found that the maximum error is 1.7% for Ri = 10.

The grid study is performed to explore the independency of the results from the grid resolution. A structured rectangular mesh was used to discretize the computational domain in this study. The impact of grid resolution on the Nusselt number of hot wall is presented in Table 2 while Ri=1, Bf =0.2, α=30° and ϕ=0.04.

It is concluded that average Nusselt number is approximately constant for the grid points finer than

Table 2. Influence of the grid resolution on the average Nusselt number.

Grid	Re=10	Re=100
	Nu_m	
40×40	5.18	17.82
60×60	4.80	17.37
80×80	4.65	17.18
100×100	4.61	17.11
120×120	4.61	17.10

Table 3. CPU Time for different Re (Ri=1, Bf=0.2, α=30°, φ=0.04).

Re	10	100	500	1000
CPU Time (Second)	1845	538	614	856

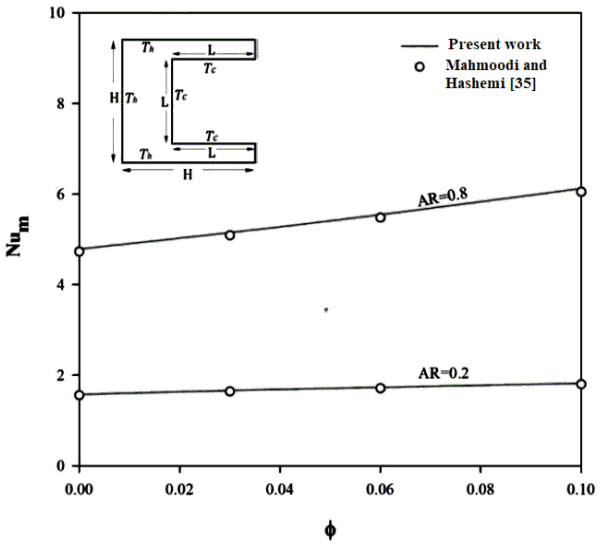

Figure 2. Average Nusselt number versus volume fraction for different aspect ratios.

100×100. Therefore, uniform grid of 100×100 was selected to perform the simulations (Figure 4). Table 3 shows the running time for Ri=1, Bf=0.2, α=30°, φ=0.04 and different Reynolds numbers. A PC with RAM of 4.00 GB and CPU core i5 2.73 GH characteristics was used to simulate the problem.

4. Results

In this section, the effect of non-dimensional parameters (Reynolds and Richardson numbers) on the flow and thermal fields, and rate of heat transfer for Bf=0.2 and α=30° are presented.

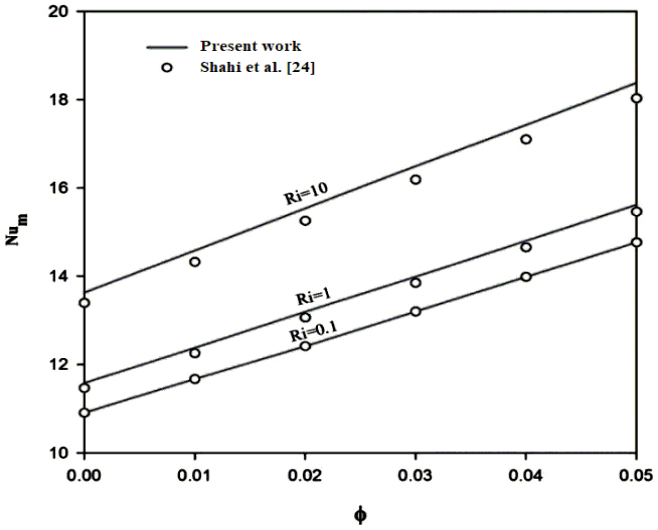

Figure 3. Average Nusselt number versus volume fraction for different Richardson numbers.

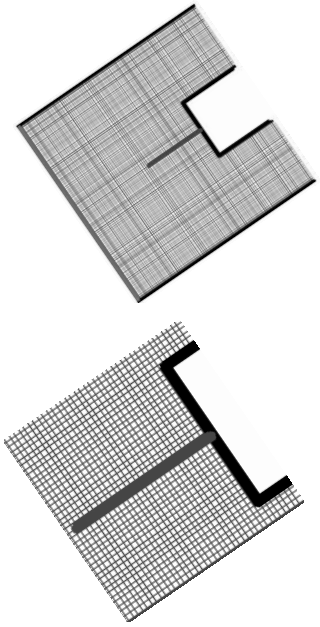

Figure 4. The grid used in the calculations of a C-shaped baffled enclosure with a zoomed-in picture around the baffle.

In Figure 5, streamlines and isothermal lines are shown at different Reynolds numbers for Ri=1. The stream functions are calculated by using the velocity field. Actually, the results of the flow filed are used to plot the streamlines by using Tecplot software. This has been done by a simple integral over the velocity components in two dimensions. The concentration of isothermal lines increases with the Reynolds number due to larger inertial effect. The figure shows that the effect of nanofluid slightly increases with the increase of Reynolds number. Streamlines are drawn toward the exit of enclosure with the increase of Reynolds number. Furthermore, isotherms were pinched to the entrance of enclosure for low values of Reynolds number due to a reduction of cold fluid flow in the entrance. Isothermal lines are drawn toward hot source with increasing of Reynolds number, indicating increase of heat transfer. Isotherms show that heat penetration into the entrance of the enclosure is higher for nanofluid flow in comparison with the pure one. This is remarkable in low Reynolds numbers, because heat diffusion is higher for nanofluid flow than the pure one.

In Figure 6, average Nusselt number is shown at different Reynolds numbers and volume fractions for Ri=1 is also presented. Increase of convection heat transfer is remarkable with increase of Reynolds number due to increase of incoming flow. At high Reynolds numbers, increase of nanoparticle has less effect on the heat transfer.

Figure 7 shows the streamlines and isotherms for pure water and nanofluid flows at different Richardson numbers and Re=100. The buoyancy force increases with increase of Richardson number. Therefore, streamlines are drawn toward the corners of enclosure. The effect of nanofluid on the streamlines increases with increase of Richardson number. Also, it is observed that isothermal lines are located at small distances from the hot wall with increase of Richardson number. On the other hand, the gradient of temperature increases with increase of Richardson numbers and results in increasing the heat transfer. The local Nusselt number at Re=100 and different Richardson numbers is shown in Figure 8. The results show that Nusselt number increases with the Richardson number due to increase of free convection heat transfer concluded from the increase of buoyancy force. It is found that the Nusselt number increases, reaches to the maximum value and then decreases.

The Nusselt number curve is approximately symmetrical at Y = 0.5 for low Richardson numbers. However, at high Richardson number of 100, the variation of the Nusselt number is different from low Richardson numbers. Average Nusselt number is shown in Figure 9 at different Richardson numbers for φ=0.04 at Re=100. The results reveal that as the Richardson number increases, average Nusselt number increases which is due to an increase of free convection heat transfer.

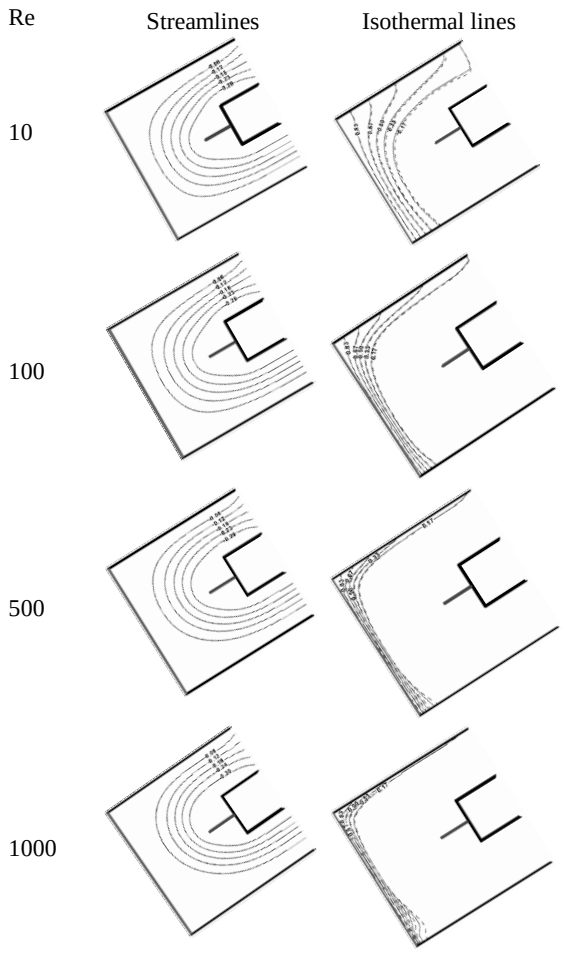

Figure 5. Streamlines and isothermal lines at different values of Reynolds number at Ri=1, for pure fluid (—) and nanofluid of φ=0.04 (- - -).

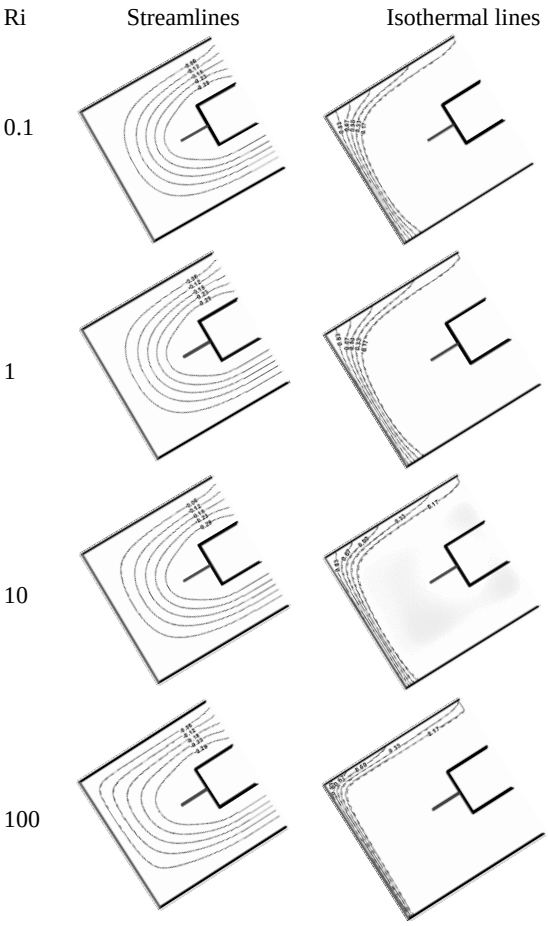

Figure 7. Streamlines and isotherms for different Richardson numbers at Re=100, for pure fluid (—) and nanofluid of φ=0.04 (- - -).

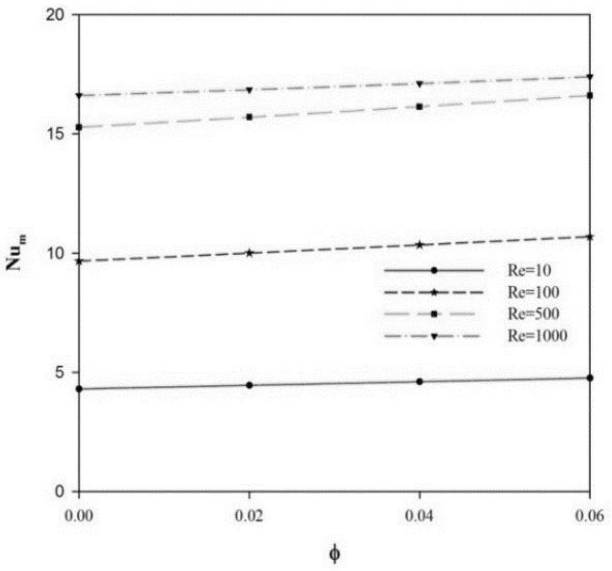

Figure 6. Average Nusselt number for different Reynolds numbers and volume fractions at Ri=1.

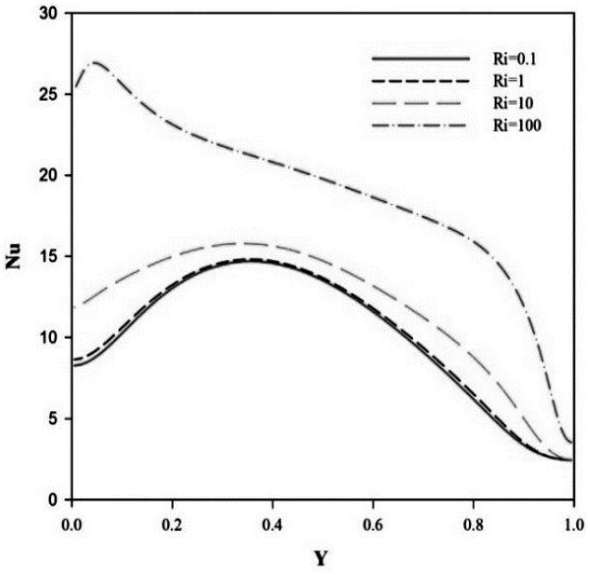

Figure 8. Effect of different Richardson numbers on the local Nusselt number at Re=100.

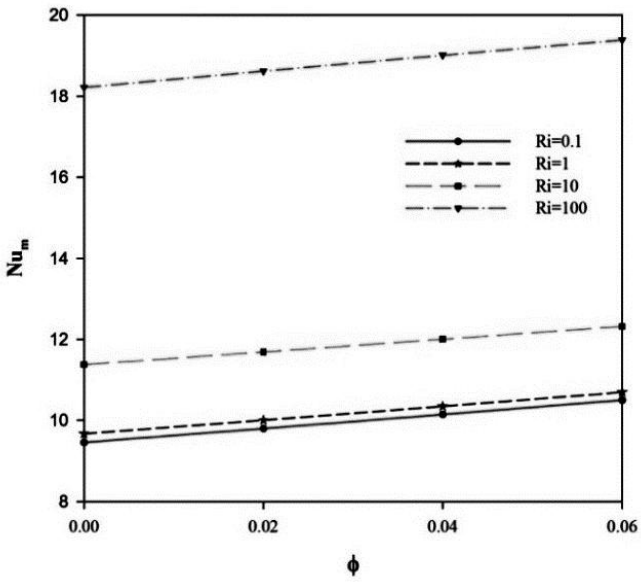

Figure 9. Effect of Richardson number and volume percent of nanoparticles on the average Nusselt number at Re=100.

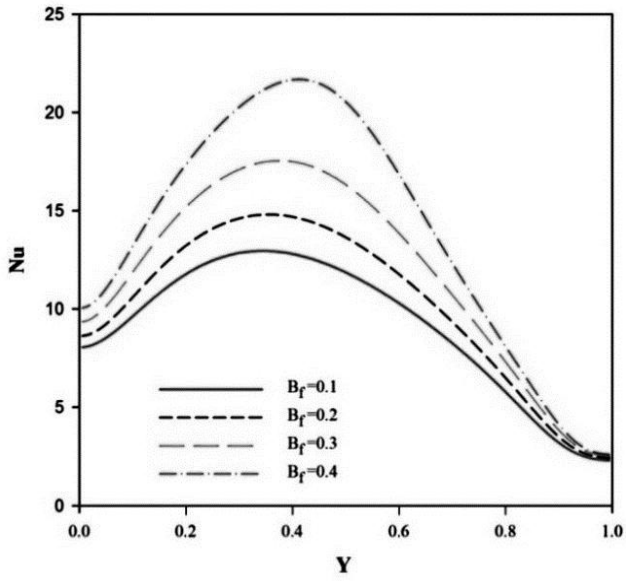

Figure 11. Effect of baffle's different length for φ=0.04 on the local Nusselt number in α=30°.

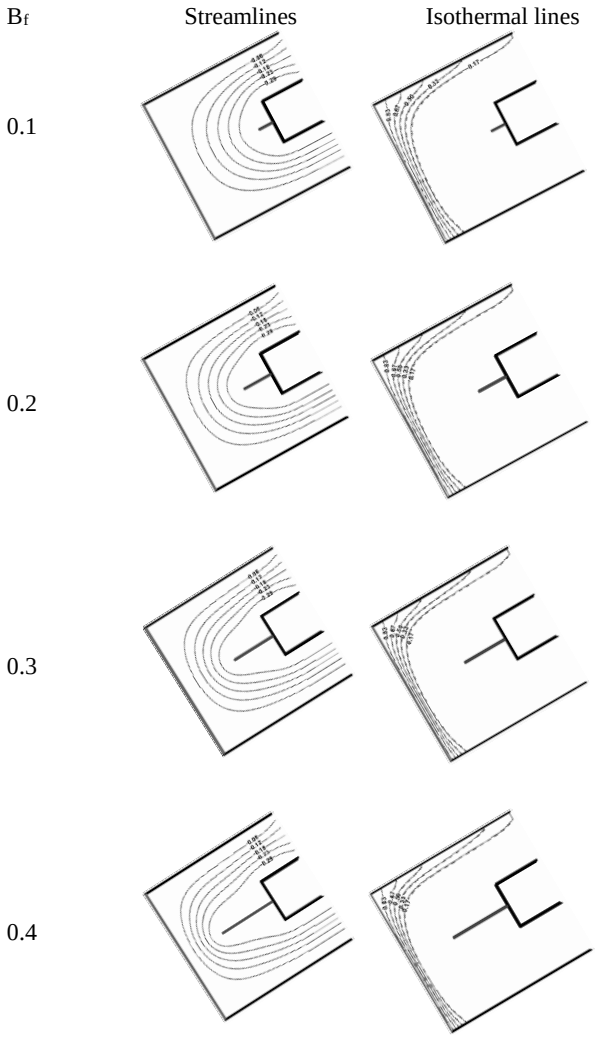

Figure 10. Streamlines and isothermal lines for different length of baffle in α=30°, for pure fluid (—) and nanofluid of φ=0.04 (- - -).

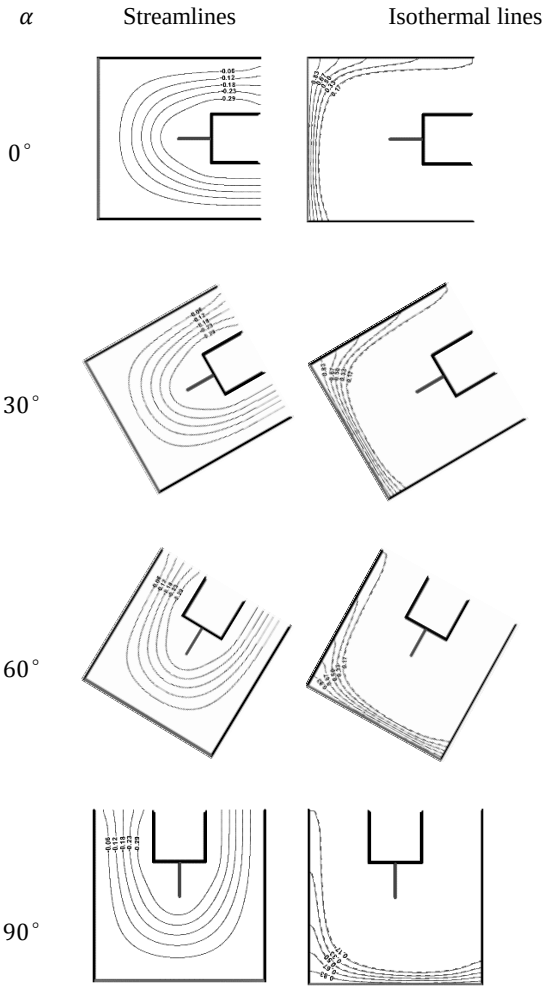

Figure 12. Streamlines and isothermal lines for different angles of enclosure in Bf =0.2, for pure fluid (—) and nanofluid of φ=0.04 (- - -).

Now, the effect of baffle length and rotation angle of enclosure on flow field and temperature field is studied for Re=100 and Ri=1. Streamlines and isothermal lines for different length of baffle are presented in Figure 10. Streamlines move toward the wall with increase of baffle length. As observed, the flow approaches the hot wall when the baffle length of enclosure increases and the space of enclosure is limited. It is concluded that this factor results in increasing the heat transfer.

The impact of baffle length of nanofluid (φ=0.04) on local Nusselt number is presented in Figure 11 for α=30°. The results show that local Nusselt number increases along hot source with increase of B_f because the space of enclosure is limited and the flow approaches the hot wall. In addition, it is observed that the main effect of baffle length on the local Nusselt number is in the middle of wall since the baffle is located in the middle of enclosure. Streamlines and isothermal lines for different angle of enclosure are shown in Figure 12 for φ=0.04 and B_f =0.2. It is observed that the concentration of isothermal lines next to the hot wall is reduced with the angle of the enclosure results in reducing heat transfer. In Figure 13, the effect of enclosure rotation and length of baffle on average Nusselt number is shown. It could be concluded that heat transfer increases as the baffle length increases. In addition, average Nusselt number decreases with increase of enclosure angle. As expected, heat transfer increases as the nanoparticles added to the pure fluid.

5. Conclusions

In the present study, mixed convection heat transfer of alumina- water in a baffled and inclined c-shape enclosure was simulated numerically. Governing equations are discretized by using finite-difference method based on the volume control and are solved by SIMPLE algorithm. Influence of non-dimensional parameters has been investigated in mixed convection hat transfer. The results indicate that the Nusselt number increases with increase of Reynolds number. Adding nanoparticles always results in cooling enclosure. At high Reynolds, increase of nanoparticles has less effect on the heat transfer. Heat transfer is an increasing function of Richardson number and baffle length. Average Nusselt number would decrease with increase of enclosure angle.

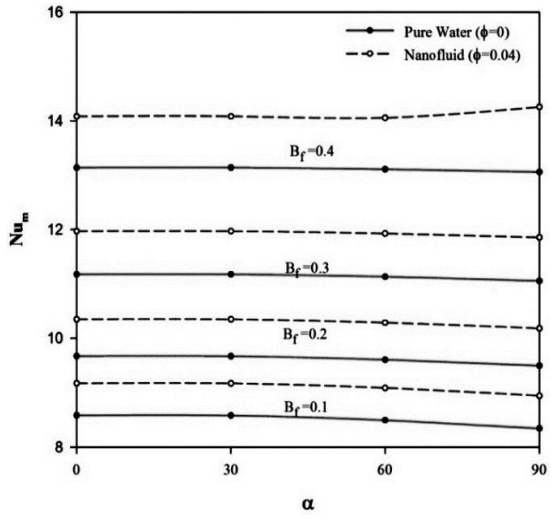

Figure 13. Effect of enclosure's rotation and length of baffle on average Nusselt number, for pure fluid (—) and nanofluid of φ=0.04 (- - -).

Nomenclature

d	Diameter, m
h	Convective heat transfer coefficient, W/m^2
k	Thermal conductivity, W/m K
L	Channel height, m
L_0	Dimensionless channel height
Nu	Nusselt number
P	Pressure, Pa
Pr	Prandtl number
Re	Reynolds number
T	Temperature, K
u, v	Velocity component, m/s
x, y	Cartesian coordinates, m

Greek letters

θ	Dimensionless temperature
μ	Dynamic viscosity, Pa.s
ν	Kinematic viscosity, Kg/m.s
ρ	Density, kg/m3
φ	Volume fraction

References

[1] Q. H. Deng, J. Zhou, C. Mei, and Y. M. Shen, heat and contaminant transport structures of laminar double-diffusive mixed convection in a two-dimensional ventilated enclosure, International Journal of Heat and Mass Transfer, 47, 5257-5269 (2004).

[2] B. Ghasemi, Mixed convection in a rectangular cavity with a pulsating heated electronic component, Numerical Heat Transfer, 47, 505-521 (2005).

[3] B. Ghasemi and S. M. Aminossadati, Numerical simulation of mixed convection in a rectangular enclosure with different numbers and arrangements of discrete heat sources, The Arabian Journal for Science and Engineering, 33, 189-207 (2008).

[4] E. Bilgen and A. Muftuoglu, cooling strategy by mixed convection of a discrete heater at its optimum position in a square cavity with ventilation ports, International

Communications in Heat and Mass Transfer, 35, 545-550 (2008).

[5] E. Sourtiji, S. F. Hosseinizadeh, M. Gorji-Bandpy and D. D. Ganji, Heat transfer enhancement of mixed convection in a square cavity with inlet and outlet ports due to oscillation of incoming flow, International Communications in Heat and Mass Transfer, 38, 806-814 (2011).

[6] N. A. C. Sidik, L. Jahanshaloo and A. Safdari, The effect of mixed convection on particle laden flow analysis in a cavity using a Lattice Boltzmann method, Computers and Mathematics with Applications, 67, 52-61 (2014).

[7] M. Najam, A. Amahmid, M. Hasanaoui, and M. E. Alami, Unsteady mixed convection in a horizontal channel with rectangular blocks periodically distributed on its lower wall, International Journal of Heat and Fluid Flow, 24, 726-735 (2003).

[8] S. M. Aminossadati and B. Ghasemi, A numerical study of mixed convection in a horizontal channel with a discrete heat source in an open cavity, European Journal of Mechanics B/Fluids, 28: 590-598 (2009).

[9] F. P. Incropera, Convection heat transfer in electronic equipment, Journal of Heat Transfer, 110: 1097–1111 (1988).

[10] G. P. Peterson, and A. Ortega, (1990) Thermal control of electronic equipment and devices, Advances in Heat Transfer, 20: 181–314.

[11] M. Najam, M. El Alami, and A. Oubarra, (2004) Heat transfer in a ‘‘T’’ form cavity with heated rectangular blocks submitted to a vertical jet: the block gap effect on multiple solutions, Energy Conversion and Management, 45: 113-125.

[12] M. Bakkas, A. Amahmid, and M. Hasanaoui, Numerical study of natural convection heat transfer in a horizontal channel provided with rectangular blocks releasing uniform heat flux and mounted on its lower wall, Energy Conversion and Management, 49, 2757-2766 (2008).

[13] S. Amraqui, A. Mezrhab, and C. Abid, Computation of coupled surface radiation and natural convection in an inclined «T» form cavity, Energy Conversion and Management, 52, 1166-1174 (2011).

[14] H. Rouijaa, M. El Alami, E. Semma, and M. Najam, Natural convection in an inclined T-shaped cavity, Tech Science Press, 7, 57-70 (2011).

[15] M. El Alami, M. Najam, E. Semma, A. Oubarra, and F. Penot, Chimney effect in a ‘‘T’’ form cavity with heated isothermal blocks: The blocks height effect, Energy Conversion and Management, 45, 3181-3191 (2004).

[16] A. Mezrhab, S. Amraqui, and C. Abid, Modeling of combined surface radiation and natural convection in a vented ‘‘T’’ form cavity, International Journal of Heat and Fluid Flow, 31, 83-92 (2010).

[17] M. Bakkas, A. Amahamid, and M. Hasanaoui, Steady natural convection in a horizontal channel containing heated rectangular blocks periodically mounted on its lower wall, Energy Conversion and Management, 47, 509-528 (2006).

[18] S. Kakaç, and A. Pramuanjaroenkij, Review of convective heat transfer enhancement with nanofluids, International Journal of Heat and Mass Transfer, 52, 3187–3196 (2009).

[19] A. Chamkha, M. Ismael, A. Kasaeipoor, and T. Armaghani, Entropy Generation and Natural Convection of CuO-Water Nanofluid in C-Shaped Cavity under Magnetic Field, Entropy, 1, 50-58 (2006).

[20] M. Ziaei-Rad and A. Kasaeipoor, A Numerical study of similarity solution for mixed-convection copper-water nanofluid boundary layer flow over a horizontal plate, Modares Mechanical Engineering, 21, 14-21 (2005).

[21] A. Kasaeipoor, B. Ghasemi, and A. RaisiMagnetic field on nanofluid water-Cu natural convection in an inclined T-shape cavity, Modares Mechanical Engineering Journal, 32, 43-49, (2014).

[22] I. Pishkar and B. Ghasemi, Cooling enhancement of two fins in a horizontal channel by nanofluid mixed convection, International Journal of Thermal Sciences, 59, 141-151 (2012).

[23] A. H. Mahmoudi, M. Shahi, and F. Talebi, Effect of inlet and outlet location on the mixed convective cooling inside the ventilated cavity subjected to an external nanofluid, International Communications in Heat and Mass Transfer, 39, 1158-1137 (2010).

[24] M. Shahi, A. H. Mahmoudi, and F. Talebi, Numerical study of mixed convective cooling in a square cavity ventilated and partially heated from the below utilizing nanofluid, International Communications in Heat and Mass Transfer, 37, 201-213 (2010).

[25] E. Sourtiji, M. Gorji-Bandpy, D. D. Ganji, and S. F. Hosseinizadeh, (2014) Numerical analysis of mixed convection heat transfer of Al2O3-water nanofluid in a ventilated cavity considering different positions of the outlet port, Power Technology, 262: 71-81.

[26] A. Kasaeipoor, B. Ghasemi and S. M. Aminossadati, Convection of Cu-water nanofluid in a vented T-shaped cavity in the

presence of magnetic field, International Journal of Thermal Sciences, 94, 50-60 (2015).
[27] N. Makulati, A. Kasaeipoor and M. M. Rashidi, Numerical study of natural convection of a water–alumina nanofluid in inclined C-shaped enclosures under the effect of magnetic field, Advanced Powder Technology, 2, 661-672 (2016).
[28] M. Siavashi, R. Yousofvand, and S. Rezanejad, Nanofluid and porous fins effect on natural convection and entropy generation of flow inside a cavity, Advanced Powder Technology, 29, 142-156 (2018).
[29] M. Siavashi, and A. Rostami, Two-phase simulation of non-Newtonian nanofluid natural convection in a circular annulus partially or completely filled with porous media, International Journal of Mechanical Science, 133, 689-703 (2017).
[30] M. Mamourian, K. Milani Shirvan, R. Ellahi, and A. B. Rahimi, Optimization of mixed convection heat transfer with entropy generation in a wavy surface square lid-driven cavity by means of Taguchi approach, International Journal of Heat and Mass Transfer, 102, 544-554 (2016).
[31] K. M. Shirvan, R. Ellahi, M. Mamourian, and M. Moghiman, Effects of wavy surface characteristics on natural convection heat transfer in a cosine corrugated square cavity filled with nanofluid, , International Journal of Heat and Mass Transfer, 107, 1110-1118 (2017).
[32] B. Ghasemi, S. M. Aminossadati and A. Rasisi, Magnetic field effect on natural convection in a nanofluid-filled square enclosure, International Journal of Thermal Science, 50, 1748-1756 (2011).
[33] J. C. Maxwell, A Treatise on Electricity and Magnetism, second ed., Oxford University Press, Cambridge (1904).
[34] H. Brinkman, The viscosity of concentrated suspensions and solutions, Journal of Chemical Physics, 20, 571-580 (1952).
[35] M. Mahmoodi and S. M. Hashemi, Numerical study of natural convection of a nanofluid in C-shaped enclosures, International Journal of Thermal Sciences, 5, 76-89 (2012).
[36] H. E. Patel, T. Sundararajan, T. Pradeep, A. Dasgupta, N. Dasgupta and S. K. Das, A micro-convection model for thermal conductivity of nanofluids, J. Phys, 65, 863-869 (2005).
[37] A. K. Santra, S. Sen and N. Chakraborty, Study of heat transfer due to laminar flow of copper-water nanofluid through two isothermally heated parallel plates, International Journal of Thermal Science, 48, 391-400 (2009).
[38] M. Sheikholeslami, M. Gorji-Bandpy, D. D. Ganji and S. Soleimani, Natural convection heat transfer in a cavity with sinusoidal wall filled with CuO–water nanofluid in presence of magnetic field, Journal of the Taiwan Institute of Chemical Engineers, 63, 10-20 (2013).
[39] S. V. Patankar, Numerical heat transfer and fluid Flow, Hemisphere Publishing Corporation, Washington D. C., (1980).